CHAPTER VIII

CHAPTER VIII

Stability of Thermally Driven Shear Flows in Long Inclined Cavities with End-to-End Temperature Difference

8.1 Introduction

During the past decade, natural convection to shallow cavities driven by an end-to-end temperature difference have received much attention. Researchers concentrated increasingly on this problem due to its relevance in several technological and fundamental areas. In the literature most of the published works considered cavities placed horizontally (Daniels and Wang(1994)). Convection in long inclined cavities driven by a temperature gradient along their longest axis is also important for a variety of phenomena that occur in industry and nature. For instance in crystal growth for vapour phase, larger transport arises. Natural convection in tilted fluid layers is also found in many geophysical situations where the fluid is enclosed in long narrow slots arbitrarily inclined to gravity. An interesting application is the transport and rate of spread of passive contaminants (for instance, radioactive material) in long tilted liquid-filled rock fractures.

In the inclined cavity of shown in the figure, the basic flow arises for any temperature difference and its intensity increases steeply with Rayleigh number as long as the isotherms are distorted by advection. The type of flow that arises is similar to that described by Woods and Linz [1996] in inclined liquid –filled rock fractures with vertical thermal gradient. Delgado –Buscalioni and Crespo del Arco (1999) studied the basic and secondary flow in an inclined cavity filled with an incompressible viscous fluid. A classical review of earlier works can be seen in the paper by Hart (1971)

Although the effect of inclined boundaries on the flow stability has been treated in a variety of geometries as far as we know, there are no published works considering the stability of the base flow in long inclined cavities with axial temperature gradient. In this chapter we investigate the stability of buoyancy driven shear flows in inclined long cavities with end wall temperature difference. Analytical expressions are found for the growth rate and stream as a function of wave number

and the stability of the flow is discussed for different inclinations and a wide range of Prandtl number.

8.2. Flow Description

We consider the flow in the two dimensional thermally driven shear flow in axially heated inclined long cavities. The cavity is filled with an incompressible viscous fluid and inclined α degrees with respect to gravity. We have employed Boussinesq approximation and assume that a convective motion is established due to a temperature difference between the end walls. That is, it is assumed that in the inclined cavity under consideration, the basic flow arises for any temperature difference and its intensity increases steeply with the Rayleigh number as long as the isotherms are distorted by advection. The geometry of the problem and the structure of the basic flow are shown below.

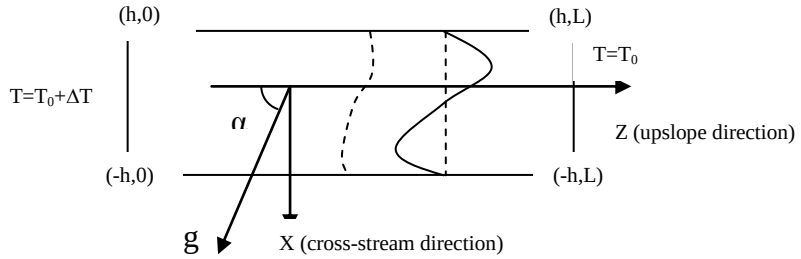

Shear flow in long inclined cavities with end to end temperature difference

In the present work, the following assumptions are made:

- Flow of a Newtonian fluid is considered, which is unsteady, viscous and laminar in nature.
- The cavity is filled with an incompressible fluid and inclined α degrees with respect to gravity
- The non slip boundary condition is used at the boundaries and the temperature in the walls $x = \pm 1$
- Boussinesq approximation is applied in the momentum equation.
- The effects of dissipation and diffusion are neglected
- Only two dimensional disturbances are considered.

The equations governing the motion are the Navier Stokes and heat transport equations with the Boussinesq approximation.

$$\nabla^* \vec{q}^* = 0 \tag{8.1}$$

$$\rho\left[\frac{\partial \vec{q}^*}{\partial t^*} + (\vec{q}^*.\nabla)\vec{q}^*\right] = -\nabla P^* - \rho^* g^* \hat{e}_g + \mu \nabla^2 \vec{q}^* \tag{8.2}$$

$$\frac{\partial T^*}{\partial t^*} + (\vec{q}^*.\nabla^*)T = k\, \nabla^{*2} T^* \tag{8.3}$$

$$\rho^* = \rho_o\,(1 - \beta_\rho * (T^* - T_o)) \tag{8.4}$$

Introducing h^2/γ, h, γ/h and ΔTh/L as scales for time, length, velocity and temperature respectively in equations (8.1) to (8.4), we get the nondimensinal equations as follows.

$$\nabla.\, \vec{v} = 0 \tag{8.5}$$

$$\frac{\partial \vec{v}}{\partial t} + (\vec{v}\,.\nabla)\vec{v} = -\nabla p + \Delta \vec{v} - RPr^{-1} T e_g \tag{8.6}$$

$$\frac{\partial T}{\partial t} + (\vec{v}\,.\nabla)T = Pr^{-1}\Delta T \tag{8.7}$$

where

$\overrightarrow{e_g} = \sin\alpha\, \hat{\imath} - \cos\alpha\, \hat{k}$, is the gravity vector.

The Rayleigh number and Prandtl number are defined respectively as $R = \frac{g\beta\Delta T h^4}{\nu k L}, and\ \mathrm{Pr} = \nu/k$.We impose the no-slip boundary conditions at all rigid boundaries and the temperature at the walls $x = \pm 1$ satisfies the homogeneous heat conduction equation.

$$\vec{v} = \vec{0} \tag{8.7}$$

$$\frac{\partial T}{\partial t} = 0 \ \ at\ \ x = \pm 1 \tag{8.8}$$

At equilibrium, we have assumed the basic velocity and temperature profiles as follows

$\vec{q}_e$ =(u_o, 0, w_o) and (8.9)

$T_o = -\eta z + b + \theta_o(x)$ (8.10)

Substituting these solutions into equations (8.3) –(8.4) and eliminating p by cross differentiation, the following system of ordinary differential equations, the following system of ordinary differential equations for $w_0(x)$ and $\theta_o(x)$ is obtained.

$R\ P_r^{-1}\eta \sin\alpha = w_o'''(x) + R\ P_r^{-1} \cos\alpha\ \theta_0(x)$ (8.11)

$P_r^{-1} v_o''(x) + \eta w_o(x) = 0$ (8.12)

With $w_o(\pm 1) = v_0'(\pm 1) = 0$ (8.13)

Solving we get

$$w_0(x) = \frac{r\tan\alpha}{Pr}\left(\frac{\sin r \sinh rx - \sinh r \sin rx}{d(r)}\right) \quad (8.14)$$

$$\theta_0(x) = -\eta\frac{\tan\alpha}{r}\left(\frac{\sin r \sinh rx + \sinh r \sin rx}{d(r)} - rx\right) \quad (8.15)$$

where

$$d(r) = \sinh r \cos r + \cosh r \sin r \quad (8.16)$$

and

$$r = (\eta R \cos\alpha)^{1/4} \quad (8.17)$$

In order to study the stability of the basic flow, we proceed in the usual form. The flow variables are written as the sum of the mean flow quantity and a small perturbation.

The stream function of the perturbation flow satisfies $u = \frac{\partial\psi}{\partial z}$, $w = -\frac{\partial\psi}{\partial x}$.

We ascribe to the stream function and temperature perturbation

$$\lambda\left(\frac{d^2}{dx^2} - k^2\right)\varphi = \left(\frac{d^2}{dx^2} - k^2\right)^2\varphi - \mathrm{ik}\left(w_o\left(\frac{\partial^2}{\partial x^2} - k^2\right)\varphi - w_o''(\varphi)\right) -$$

$$R P_r^{-1}(ik\sin\alpha\theta + \cos\alpha\theta') \quad (8.18)$$

$$\lambda\theta = P_r^{-1}\left(\frac{d^2}{dx^2} - k^2\right)\theta - \mathrm{ik}\left(\theta_o'\varphi + w_o\theta\right) - \psi' \quad (8.19)$$

Boundary conditions are $\varphi(\pm1) = \varphi'(\pm1) = 0, \quad \theta'(\pm1) = 0$ (8.20)

Equations (8.18)-(8.20) have non trivial solutions only for certain values of the frequency parameter λ (eigen values). The boundary value problem is not self adjoint. Hence in general the frequency of the disturbances λ will admit complex values which will determine the stability of the problem.

8.3 Analysis

In this section we analyse the behavior of the disturbances for long waves i.e., k is assumed to be small. We attempt to find analytical expressions for the growth rate and stream using regular perturbation method.

Assuming

$$\lambda = \lambda_o + k^2 \lambda_1 + \ldots..$$

$$\theta = T_o + kT_1 + k^2 T_2 + \ldots\ldots$$

$$\varphi = \varphi_o + k\,\varphi_1 + k^2 \varphi_2 + \ldots\ldots. \quad (8.21)$$

Substituting (8.21) in (818) –(8.20)

$$(\lambda_o + k^2 \lambda_1 + \ldots..)\left(\frac{\partial^2}{\partial x^2} - k^2\right)(\varphi_o + k\,\varphi_1 + k^2 \varphi_2 + \ldots\ldots.)$$

$$= \left(\frac{\partial^4}{\partial x^4} - 2k^2 \frac{d^2}{dx^2} + k^4\right)(\varphi_o + k\,\varphi_1 + k^2 \varphi_2 + \ldots\ldots.)$$

$$-ik\left\{w_o\left(\frac{d^2}{dx^2} - k^2\right)(\varphi_o + k\varphi_1 + k^2\varphi_2 + ...) - w''_o(\varphi_o + k\varphi_1 + k^2\varphi_2 + ...)\right\}$$

$$- R\,P_r^{-1} ik \sin\alpha\left[T_o + kT_1 + k^2 T_2 + ...\right]$$

$$- R\,P_r^{-1} \cos\alpha\left[\frac{dT_o}{dx} + k\frac{dT_1}{dx} + k^2\frac{dT_2}{dx} + ...\right] \quad (8.22)$$

$$(\lambda_o + k^2 \lambda_1 + \ldots..)\left[T_o + kT_1 + k^2 T_2 + ...\right]$$

$$= P_r^{-1}\left(\frac{d^2}{dx^2} - k^2\right)\left[T_o + kT_1 + k^2 T_2 + ...\right]$$

$$-ik\,\theta'_o\ (\varphi_o + k\varphi_1 + k^2\varphi_2 + ...)$$

$$-\mathrm{ik}\, w_o \ (\theta_o + k\theta_1 + k^2\theta_2 + ...) \qquad (8.23)$$

Collecting various order of k, the equations governing the velocity and temperature perturbations are given by

$$\left[P_r^{-1} \frac{d^4}{dx^4} - \lambda_o (P_r^{-1} + 1) \frac{d^2}{dx^2} + (\lambda_o^2 - R P_r^{-1} \cos\alpha) \right] \varphi_o = 0$$

$$\left[\frac{d^4}{dx^4} - \lambda_o \frac{d^2}{dx^2} \right] \varphi_1 = \lambda_1 \frac{d^2\varphi_o}{dx^2} + i \left[w_o \frac{d^2\varphi_0}{dx^2} - w_o'' \varphi_o \right] + i R P_r^{-1} \sin\alpha \ \ t_o + R P_r^{-1} \cos\alpha \ \ t_1'$$

$$\left(\frac{\partial^4}{\partial x^4} - \lambda_0 \frac{d^2}{dx^2} \right) \varphi_2 = \lambda_1 \frac{d^2\varphi_0}{dx^2} - \varphi_0 \lambda_0 + 2 \frac{d^2\varphi_0}{dx^2} + i w_0 \frac{d^2\varphi_1}{dx^2} - w_0'' + RPr^{-1} \sin\alpha T_1 + RPr^{-1} \cos\alpha T_2'$$

$$\lambda_o T_o = P_r^{-1} \frac{d^2 T_o}{dx^2} - \frac{d\varphi_o}{dx}$$

$$\left(Pr^{-1} \frac{d^2 T_2}{dx^2} - \lambda_0 T_2 \right) = \lambda_1 T_0 + T_0 Pr^{-1} + i\left(\theta_0' \varphi_1 + w_0 T_1\right) + \varphi_2'$$

Boundary conditions $\varphi_o(\pm 1) = 0, \quad \varphi_o'(\pm 1) = 0, \ \mathrm{T_o}(\pm 1) = 0 \qquad (8.24)$

Solving we get

$$\varphi_o = \cosh(x) + \mathrm{A_1} \cosh(\mathrm{R_2 x})$$

$$\mathrm{T_o} = \mathrm{A_2} \cosh(\sqrt{\lambda_o P_r}\, x) + \mathrm{A_3} \sinh(\sqrt{\lambda_o P_r}\, x) + \frac{R_1}{P_r^{-1} R_1^2 - \lambda_o} \sinh(R_1 x) + \frac{R_2 A_1}{P_r^{-1} R_2^2 - \lambda_o} \sinh(R_2 x)$$

Applying the boundary conditions we get the eigenvalues and eigen functions as follows.

$$R_2 \sinh(R_1)\cosh(R_2) - R_1 \sinh(R_2)\cosh(R_1) = 0$$

$$R_2 \cosh(R_1)\sinh(R_2) - R_1 \cosh(R_2)\sinh(R_1) = 0 \qquad (8.25)$$

The above expressions do not give explicit values for λ_0. Hence the values of λ_0 are obtained using the software Mathematica 8.0.

$$\begin{aligned}\varphi_1 = {} & A_5\cosh(R_1x) + A_6\sinh(R_1x) + A_7\cosh(R_2x) + A_8\sinh(R_2x) \\ & + A_9\lambda_1\cosh(\sqrt{\lambda_o P_r}x) \\ & + A_{10}\lambda_1 x \sinh(R_1x) \\ & + A_{11}\lambda_1 x \sinh(R_2x) \\ & + A_{12} x\cosh(R_1x) + A_{13} x\cosh(R_2x) \\ & + A_{14}\sinh((r+R_1)x) + A_{15}\sinh((r-R_1)x) \\ & + A_{16}\sinh((r+R_2)x) + A_{17}\sinh((r-R_2)x) \\ & + A_{18}\sin((r+iR_1)x) + A_{19}\sin((r-iR_1)x) \\ & + A_{20}\sinh((r+iR_2)x) + A_{21}\sinh((r-iR_2)x) \\ & + A_{22}\sinh((r+\sqrt{\lambda_o P_r})x) + A_{23}\sinh((r-\sqrt{\lambda_o P_r})x) \\ & + A_{24}\sinh((r-i\sqrt{\lambda_o P_r})x) + A_{25}\sinh((r+i\sqrt{\lambda_o P_r})x) \qquad (8.26)\end{aligned}$$

For brevity, the constants are given in *Appendix B.*

8.4. Results and Discussion

We consider the flow in the two dimensional thermally driven shear flow in axially heated inclined long cavities. The cavity is filled with an incompressible viscous fluid and inclined α degrees with respect to gravity. We have employed Boussinesq approximation and assume that a convective motion is established due to a temperature difference between the end walls. The effect of inclined boundaries on the stability of the basic flow in axially heated long inclined cavity is the main concern of this section. Hence we have found the value of the growth rate as a function of Prandtl number, Rayleigh number and angle of inclination numerically and plotted them in figures (8.1) –(8.6).

It was found from these figures that Rayleigh number plays a significant role in enhancing the stability of the flow. We can see that the real part of the growth rate decreases due to increase in Rayleigh number. Angle of inclination and Prandtl number is found to increase the growth rate.

Figures (8.7) – (8.10) it can be seen that increase in angle of inclination, Prandtl number and the wave number are found to decrease the stream function of the disturbances. Hence we can infer that by increasing the angle of inclination we can stabilize the flow.

Figures (8.11) –(8.18) it can be seen that temperature profile increases with the increase in the Rayleigh number, Prandtl number and wave number. Increase in the angle of inclination of the cavity decreases the temperature of the flow.

8.5 Conclusions

Since we find no published analytical works considering the stability of the base flow in long inclined cavities with axial temperature gradient, in this chapter we investigated the stability of buoyancy driven shear flows in inclined long cavities with end wall temperature difference. Analytical expressions are found for the growth rate and stream as a function of wave number and the stability of the flow is discussed for different inclinations and a wide range of Prandtl number.

Some of the important finding are

- Rayleigh number plays a significant role in enhancing the stability of the flow. Real part of the growth rate decreases due to increase in Rayleigh number.
- Angle of inclination and Prandtl number are found to increase the growth rate.
- Increase in angle of inclination, Prandtl number and the wave number are found to decrease the stream function
- Temperature profile increases with the increase in the Rayleigh number, Prandtl number and wave number.
- Increase in the angle of inclination of the cavity decreases the temperature of the flow.

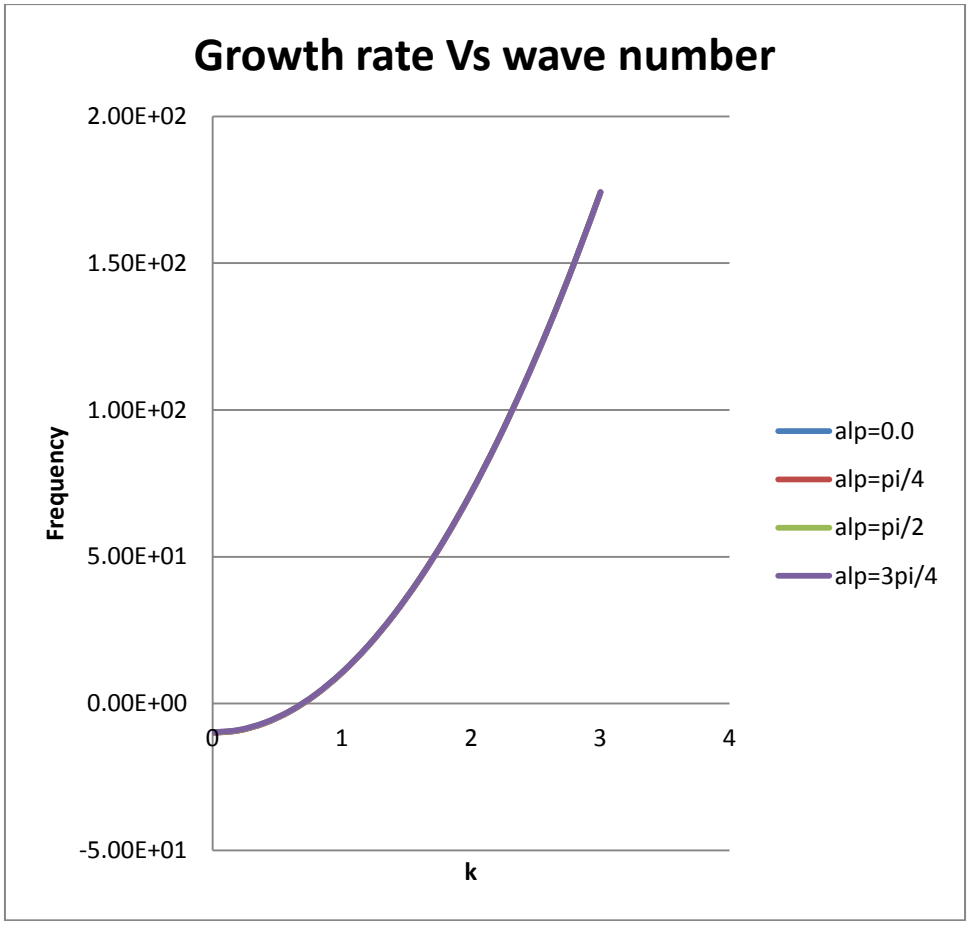

Figure 8.1 Growth rate as a function of wave number (Pr =0.7, R=10.0)

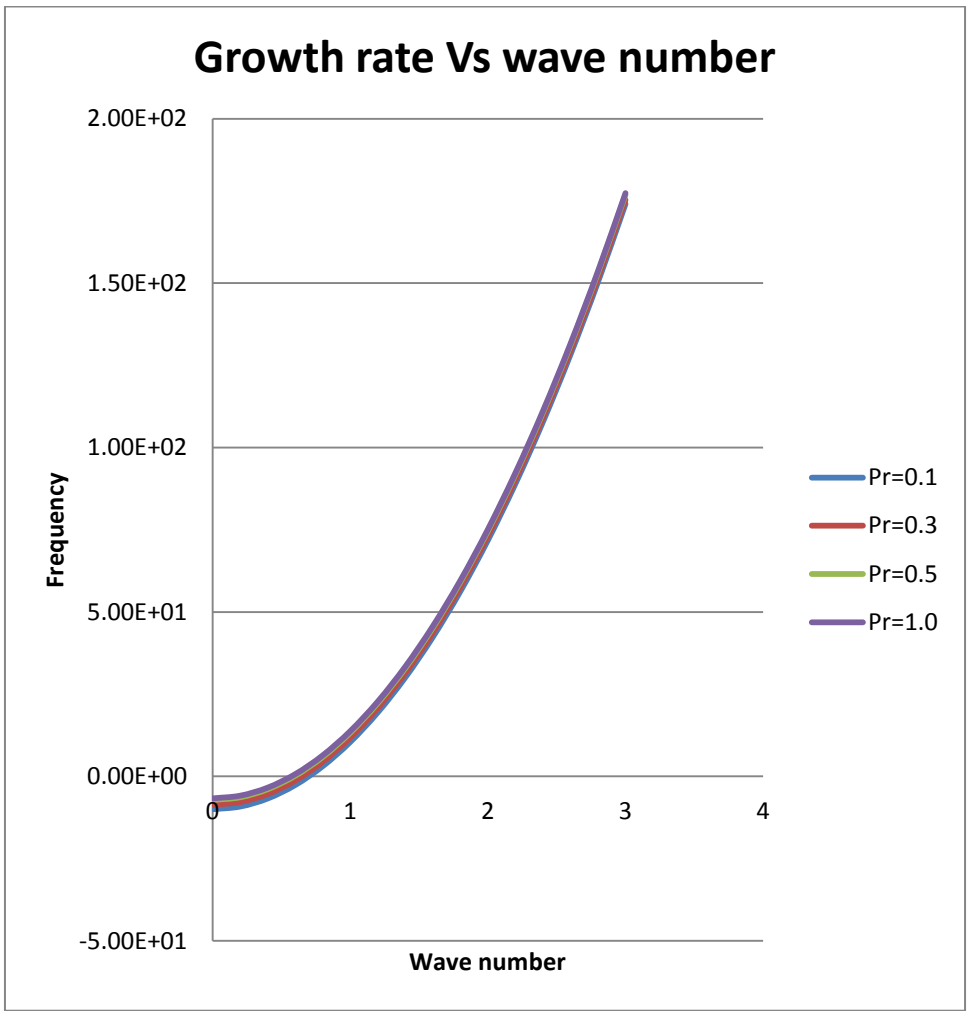

Figure 8.2 Growth rate as a function of wave number (alpha = pi/3.0, R=10.0)

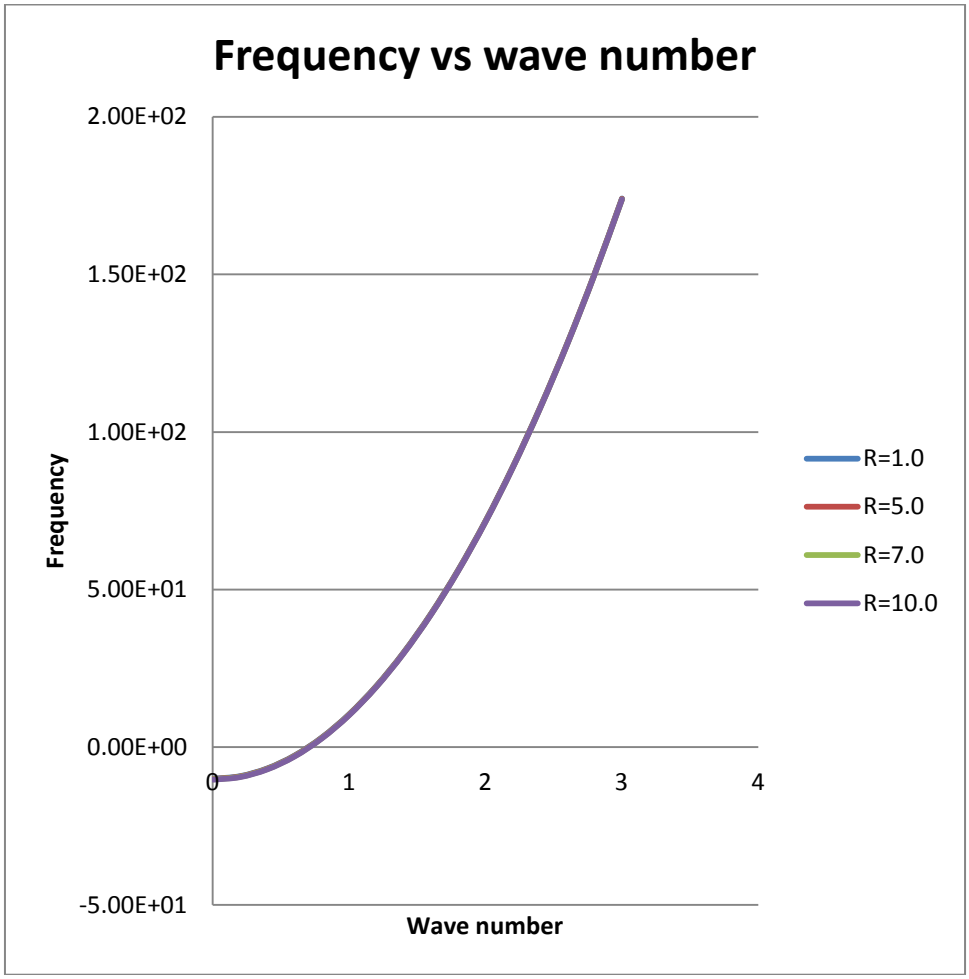

Figure 8.3 Growth rate as a function of wave number (alpha = pi/6.0, Pr=0.7)

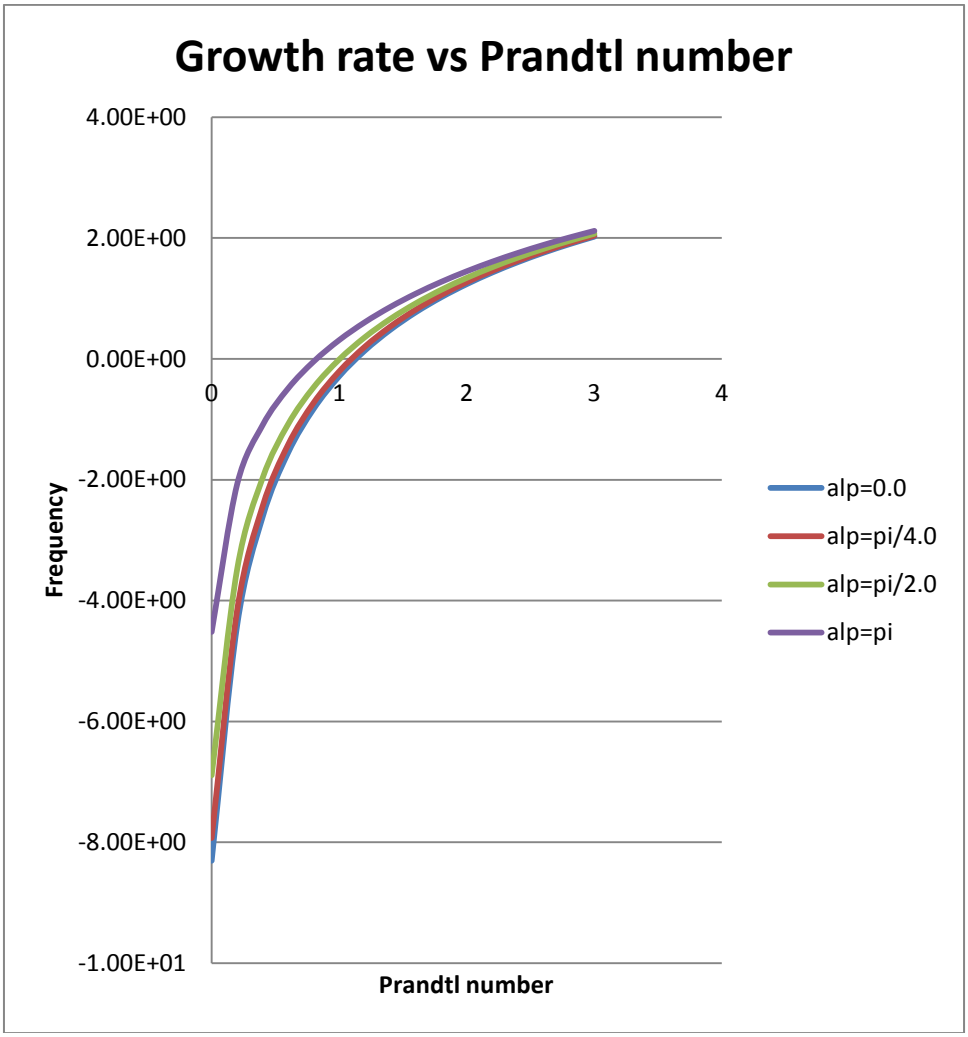

Figure 8.4 Growth rate variation with respect to Prandtl number (alpha = pi/6.0,R=10.0)

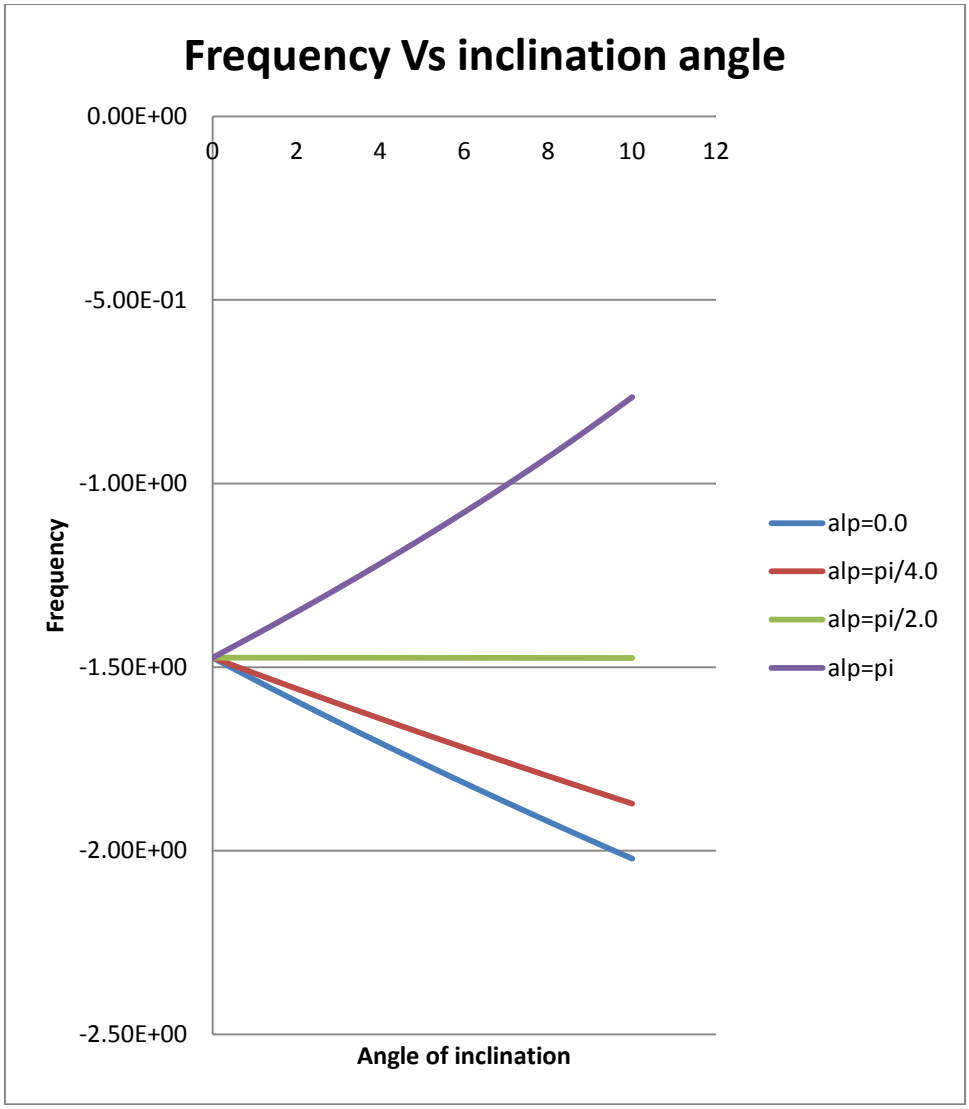

Figure 8.5 Growth rate variation with respect to Angle of inclination (Pr=0.7,R=10.0)

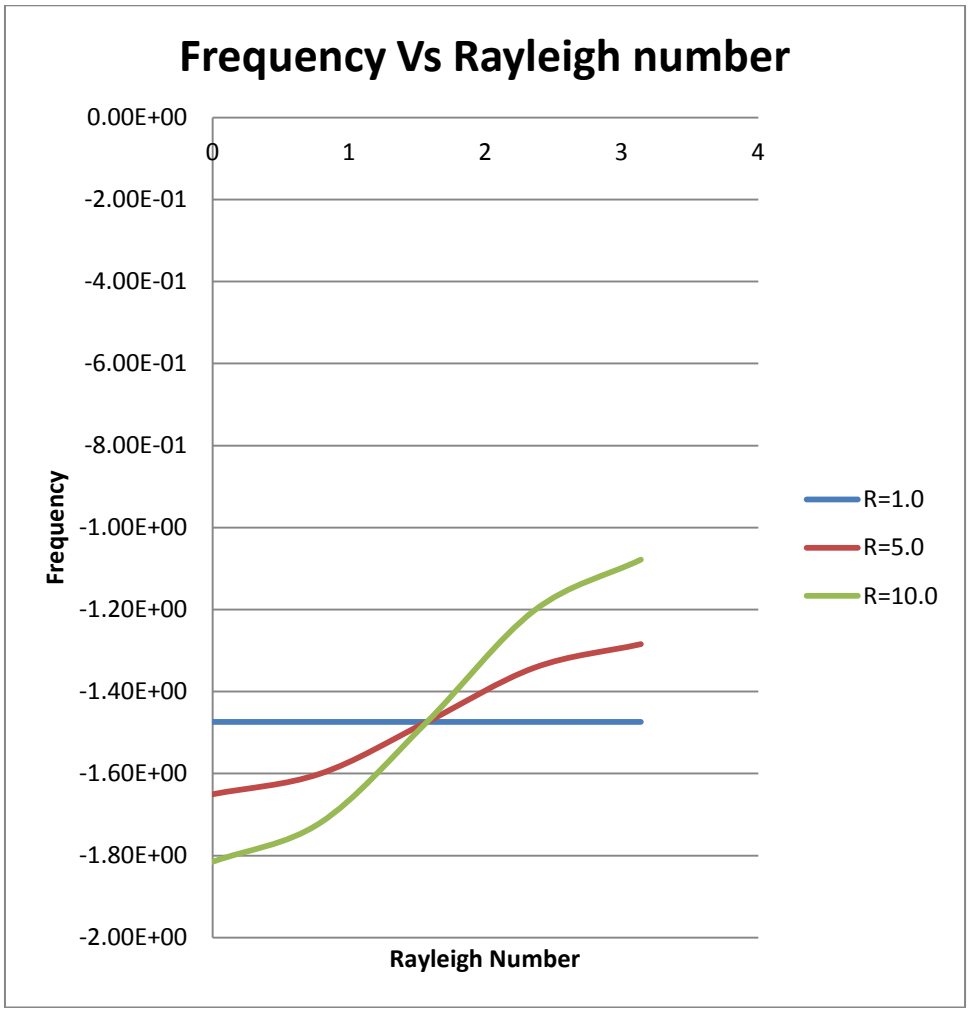

Figure 8.6 Growth rate variation with respect to R (Pr=0.7,alpha=pi/3)

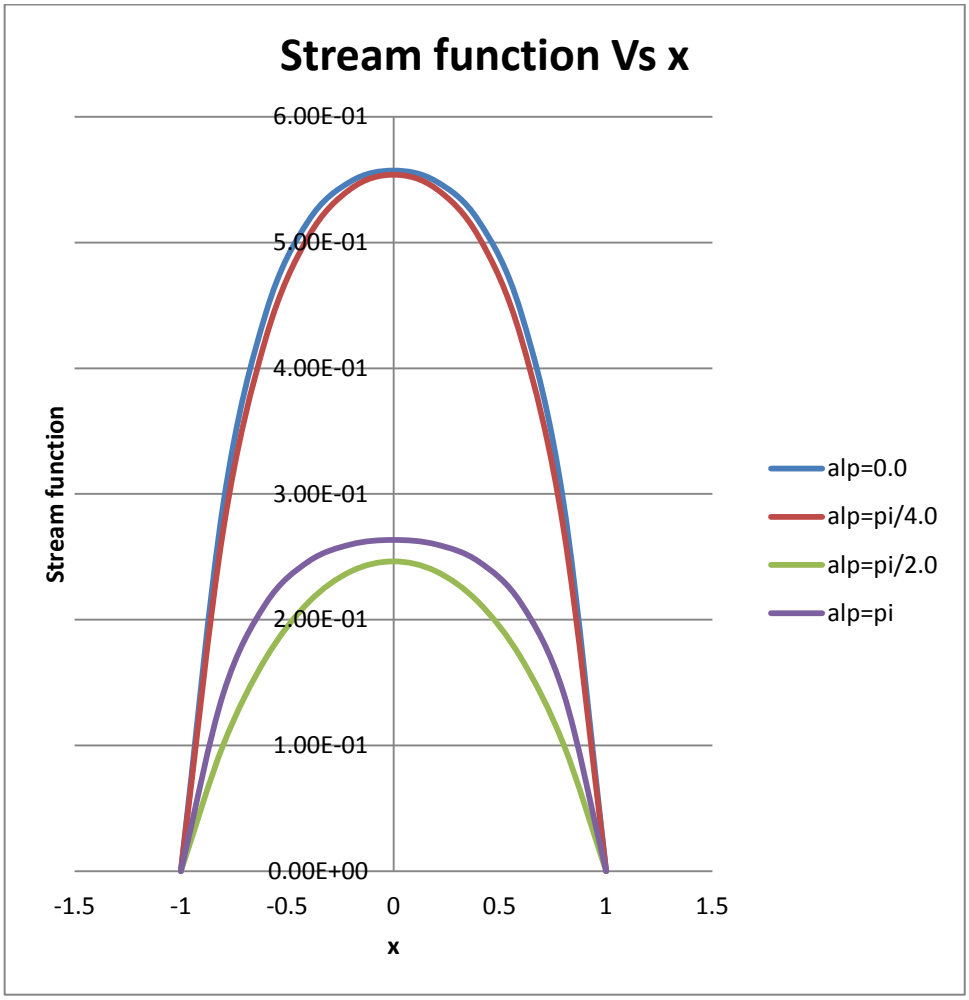

Figure 8.7 Stream function variation wrt x (Pr=0.7, R=10.0)

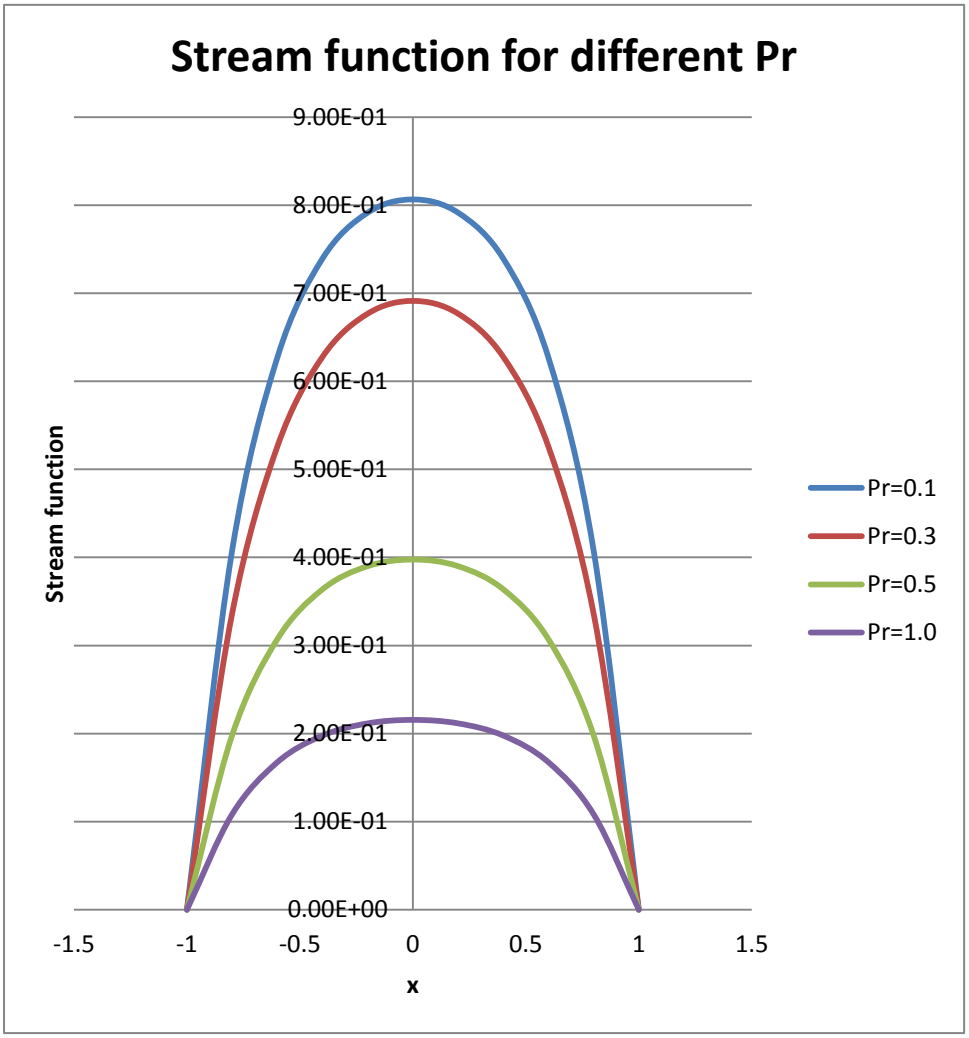

Figure 8.8 Stream function variation wrt x (alp=pi/3,R=10.0)

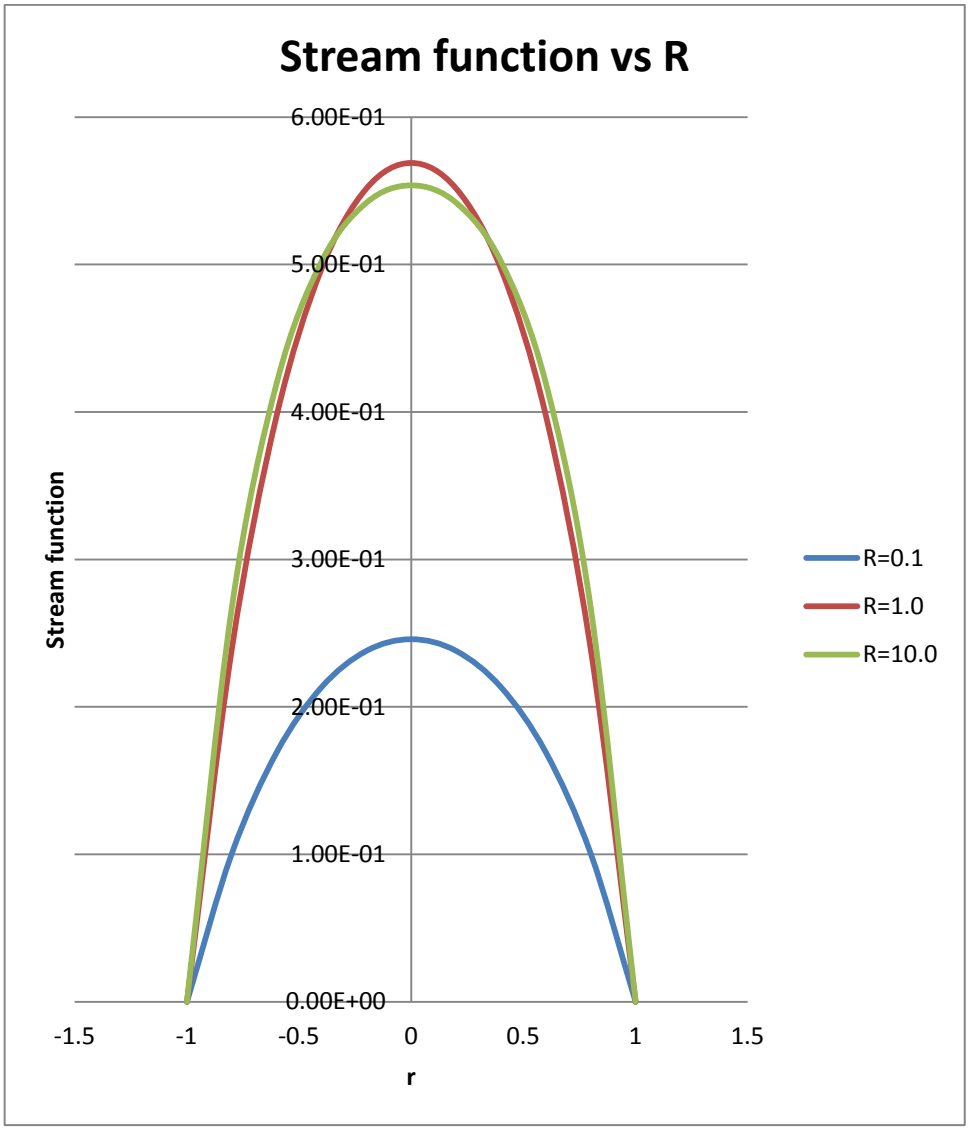

,

Figure 8.9 Stream function variation wrt x (alp=pi/3,Pr= 0.7)

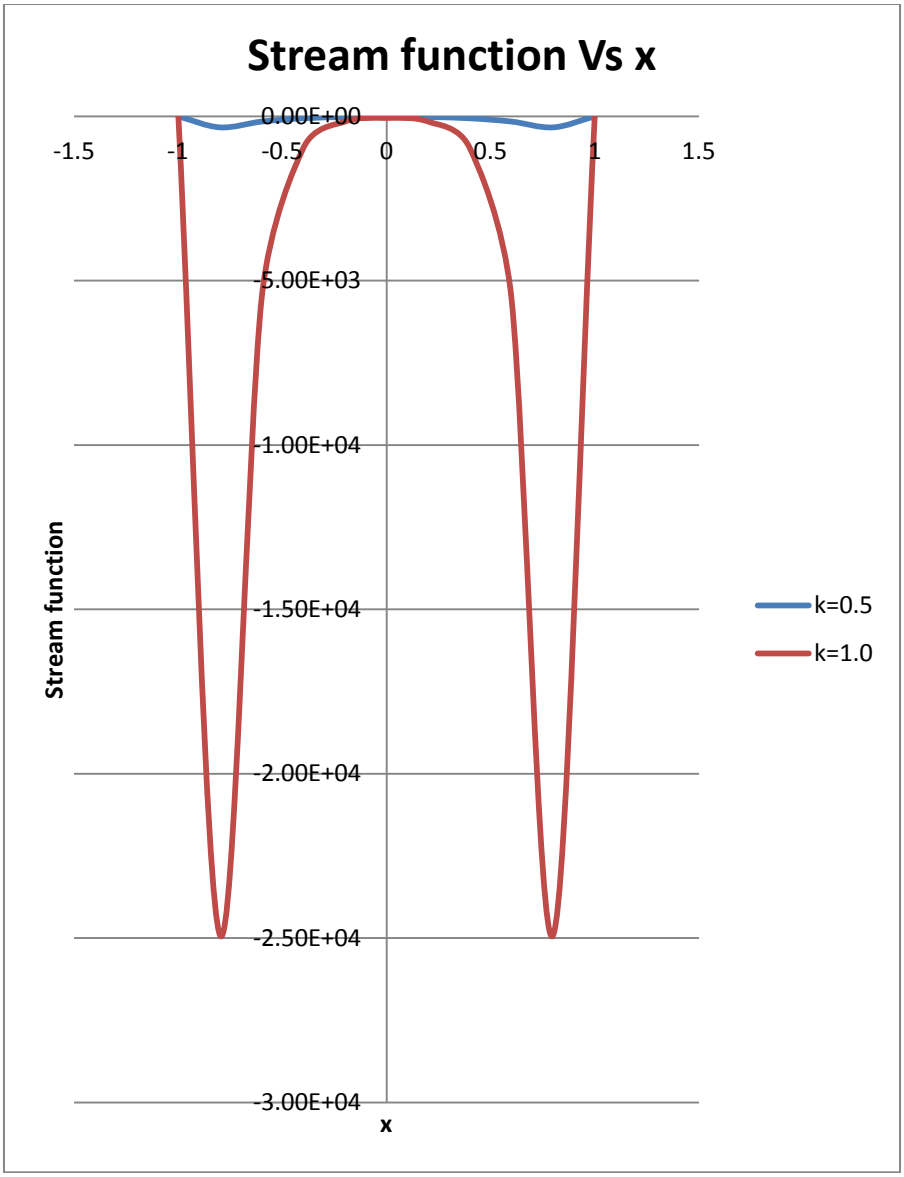

Figure 8.10 Stream function variation wrt x (alp=pi/3,Pr=0.7, R=10.0)

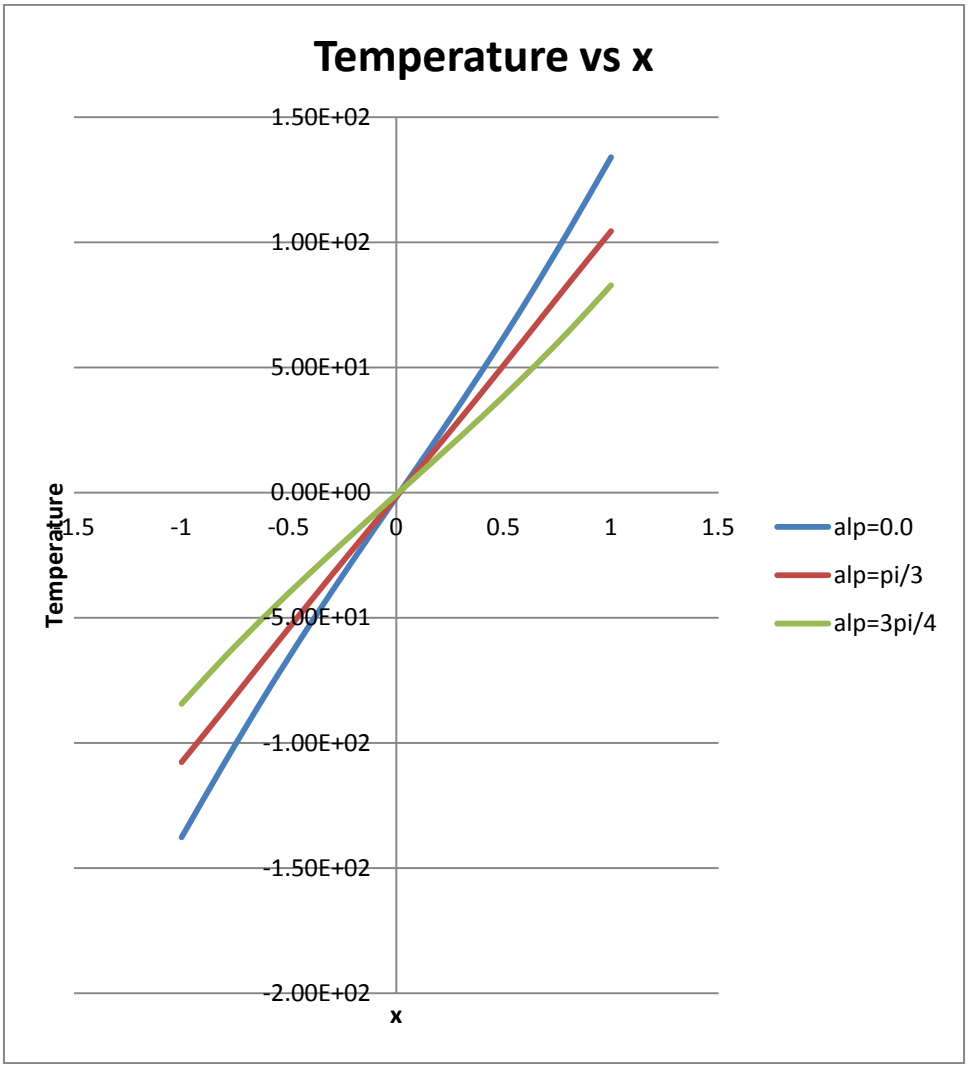

Figure 8.11 Temperature distribution as a function of x (k=0.5,Pr=0.7, R=10.0)

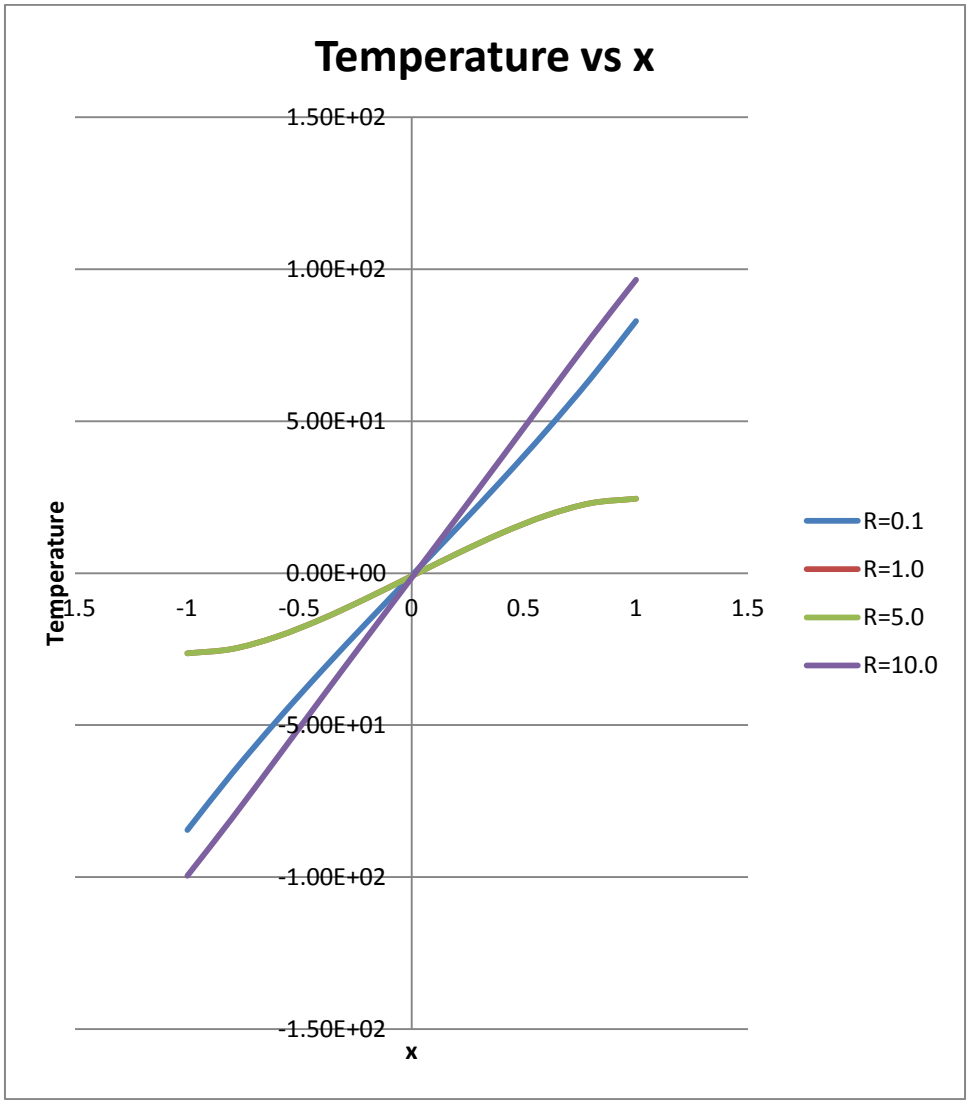

Figure 8.12 Temperature distribution as a function of x (k=0.5,Pr=0.7, alp = pi/6)

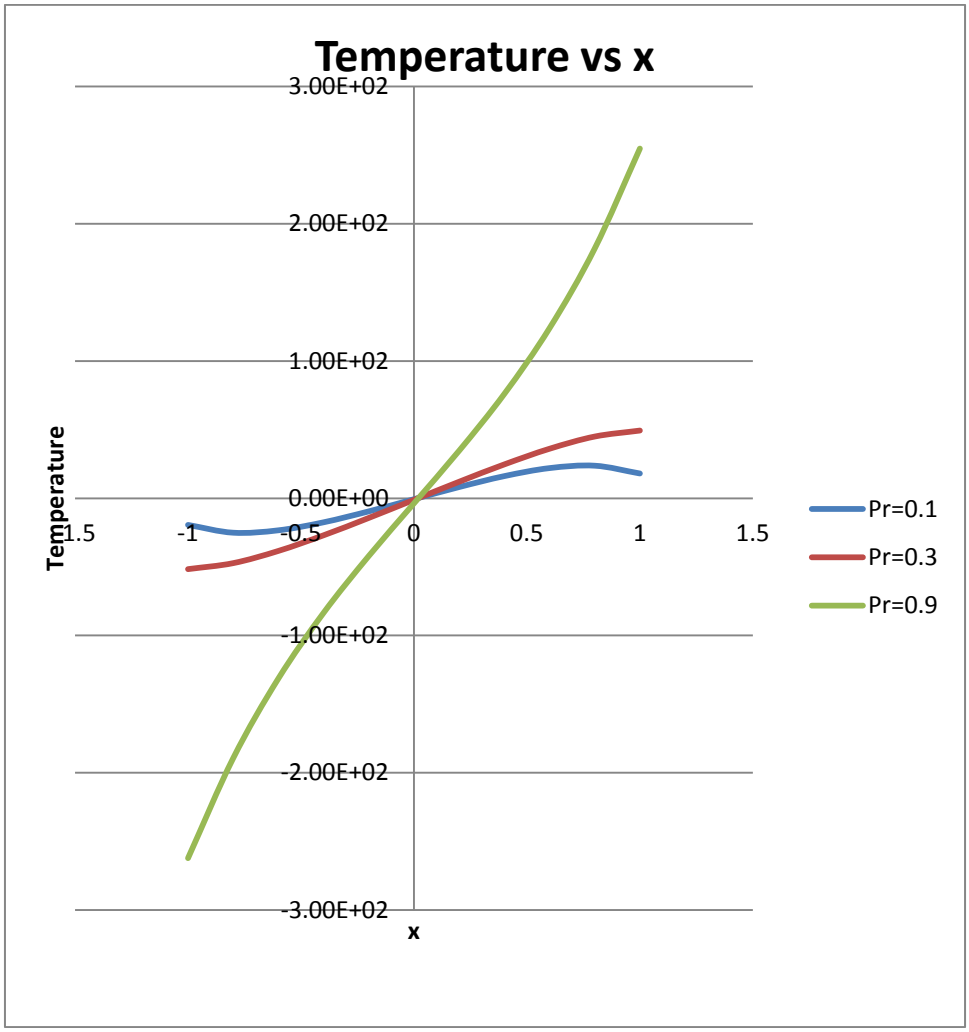

Figure 8.13 Temperature distribution as a function of x (k=0.5,R=10.0, alp = pi/6)

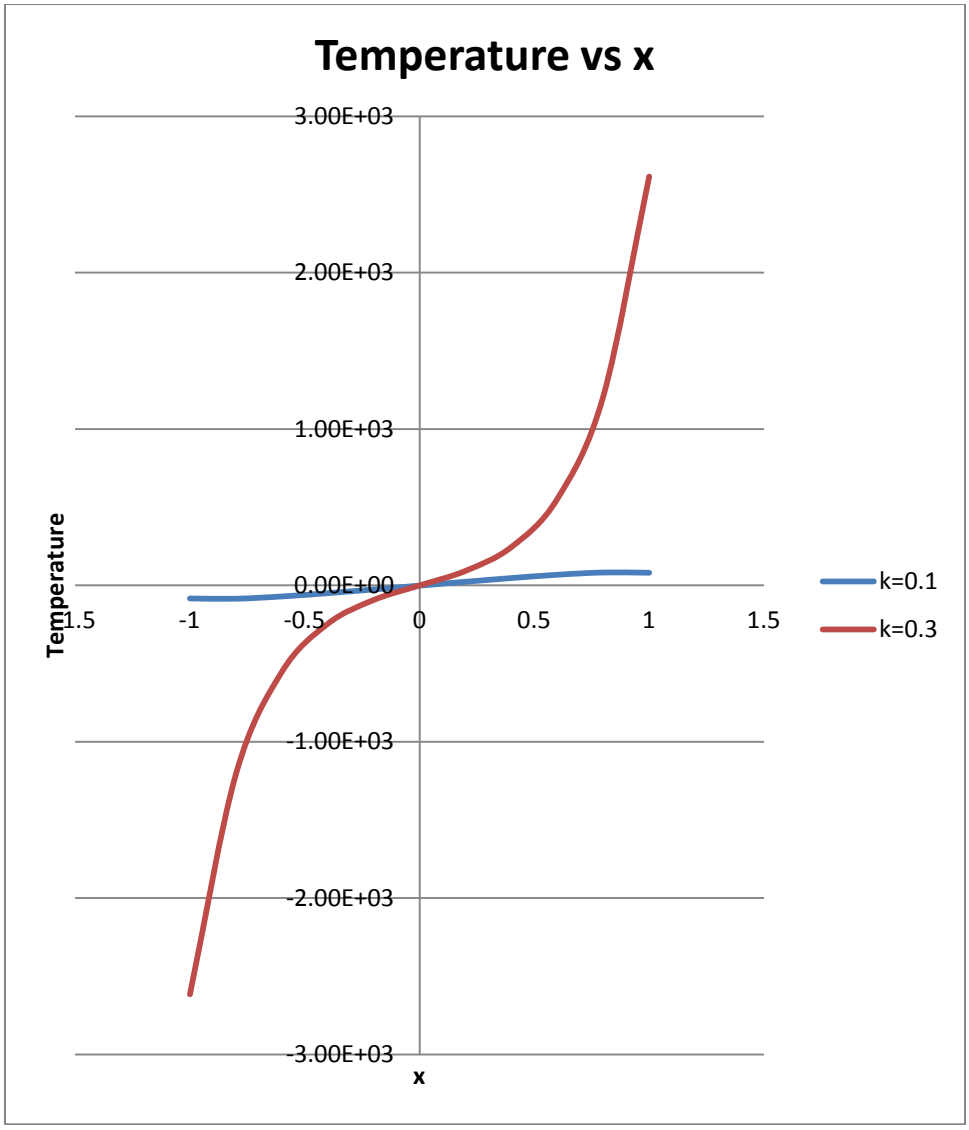

Figure 8.14 Temperature distribution as a function of x (Pr=0.7, R=10.0, alp = pi/6)

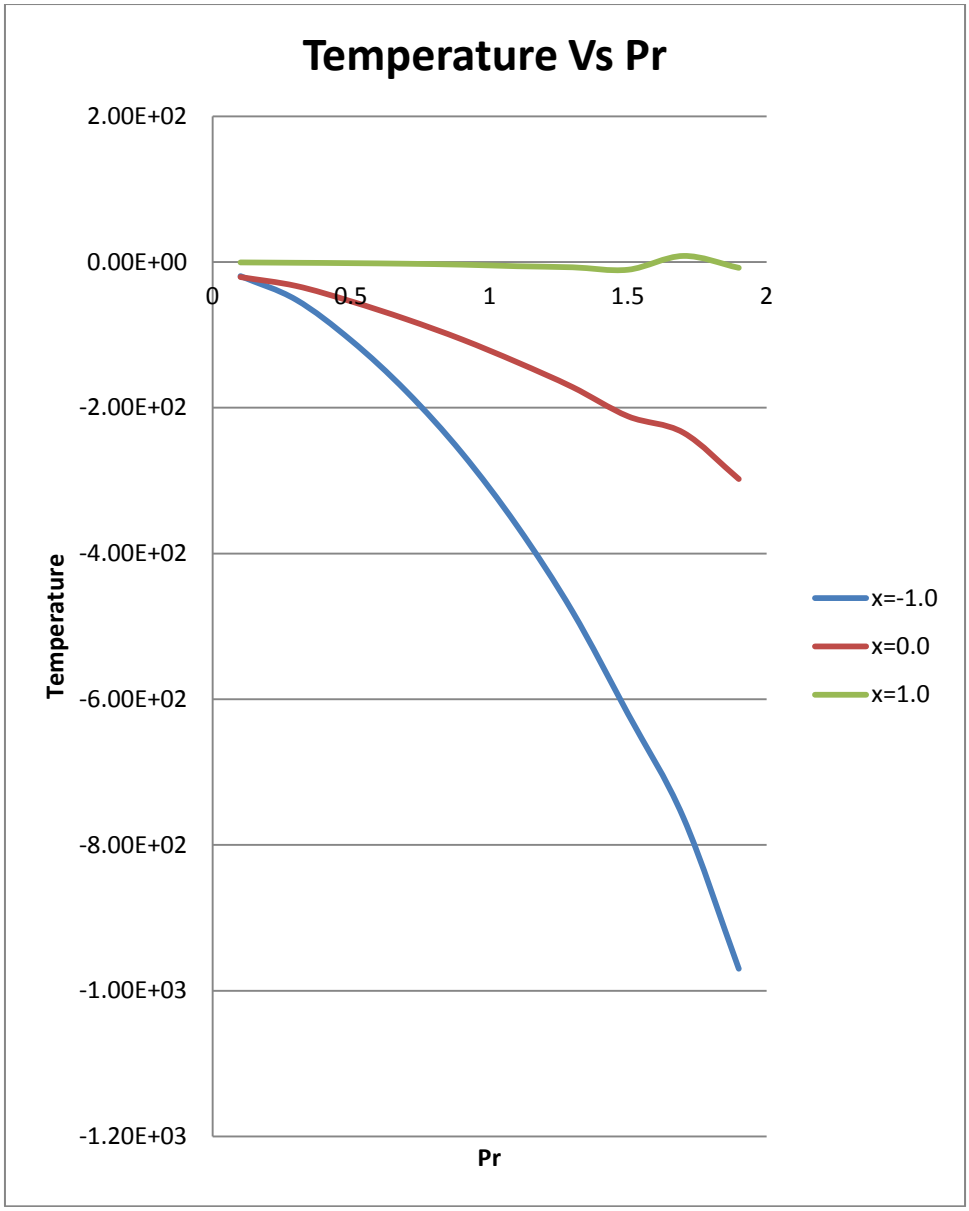

Figure 8.15 Temperature distribution as a function of Pr (k=0.4,R=10.0, alp = pi/6)

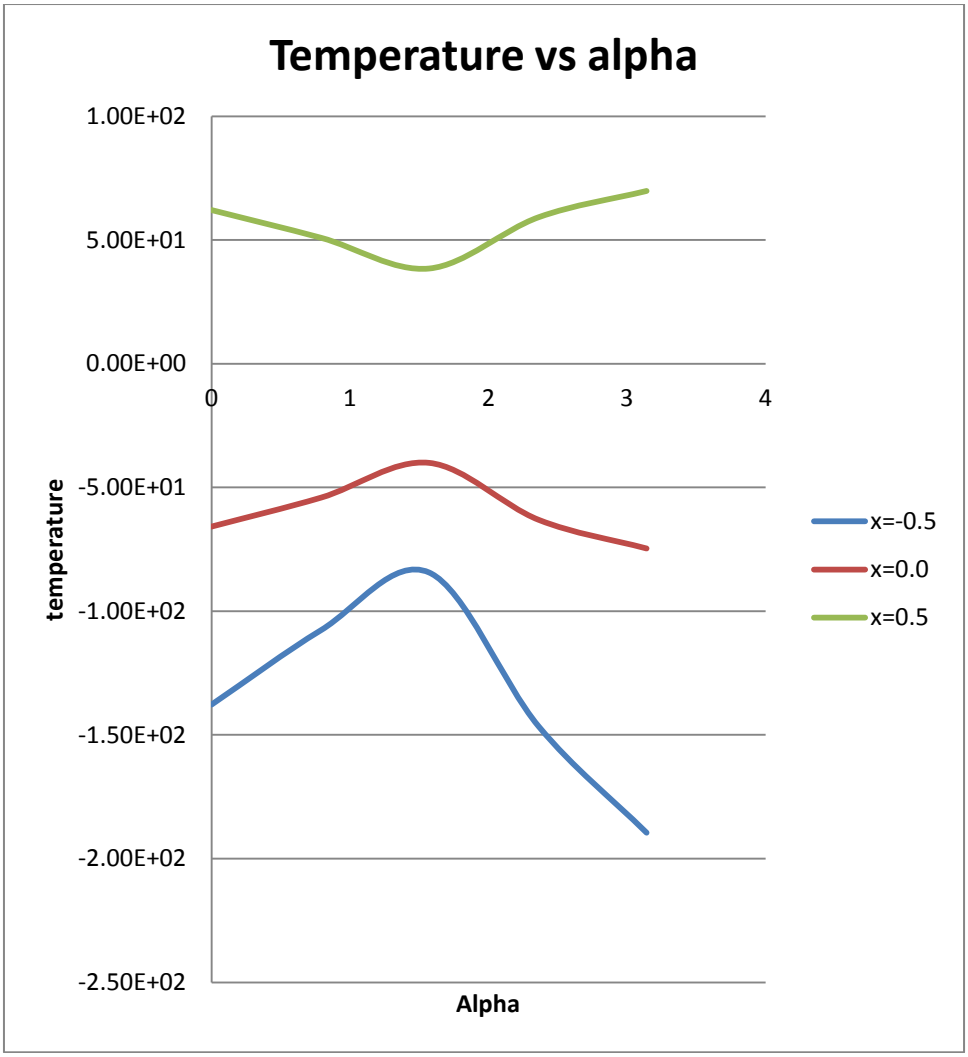

Figure 8.16 Temperature distribution as a function of alpha (k=0.4,R=10.0, Pr=0.71)

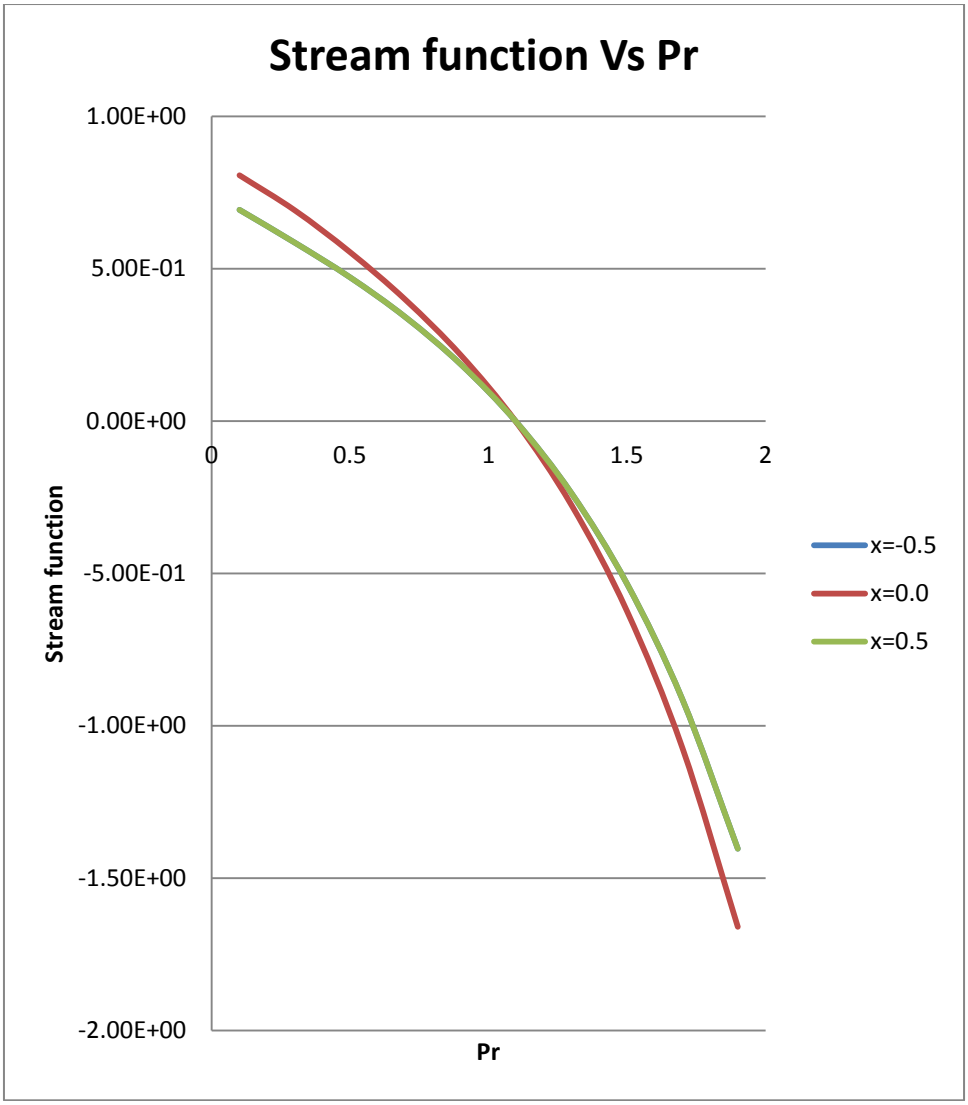

Figure 8.17 Stream function as a function of Pr (k=0.4,R=10.0, alp=pi/6.0)

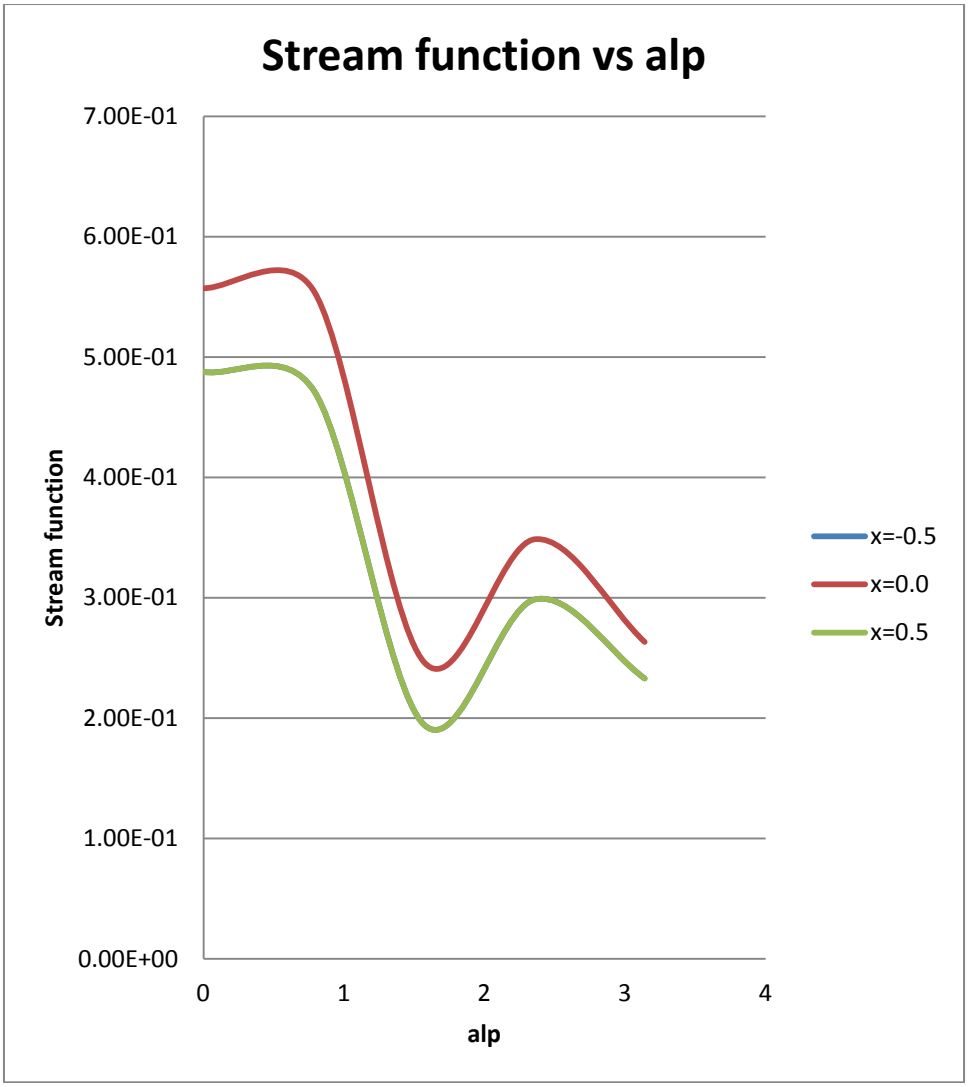

Figure 8.18 Stream function as a function of alpha (k=0.4,R=10.0, Pr = 0.71)